Genes & Diseases (2023) 10, 1596–1612

Available online at www.sciencedirect.com

ScienceDirect

journal homepage: www.keaipublishing.com/en/journals/genes-diseases

FULL LENGTH ARTICLE

Hepatocyte nuclear factor 1A suppresses innate immune response by inducing degradation of TBK1 to inhibit steatohepatitis

Jinyong He [a,b,c,d,1], Cong Du [a,b,c,1], Xuyun Peng [a,b,c], Weilong Hong [e], Dongbo Qiu [a,b,c], Xiusheng Qiu [a,b,c], Xingding Zhang [d,**], Yunfei Qin [a,b,c,**], Qi Zhang [a,b,c,*]

[a] *Cell-gene Therapy Translational Medicine Research Center, The Third Affiliated Hospital, Sun Yat-sen University, Guangzhou, Guangdong 510630, China*
[b] *Biotherapy Center, The Third Affiliated Hospital, Sun Yat-sen University, Guangzhou, Guangdong 510630, China*
[c] *Guangdong Province Key Laboratory of Liver Disease Research, The Third Affiliated Hospital, Sun Yat-sen University, Guangzhou, Guangdong 510630, China*
[d] *Molecular Cancer Research Center School of Medicine, Sun Yat-sen University, Shenzhen, Guangdong 518107, China*
[e] *Department of Emergency, The Third Affiliated Hospital, Sun Yat-sen University, Guangzhou, Guangdong 510630, China*

Received 22 December 2021; received in revised form 5 May 2022; accepted 26 May 2022
Available online 7 June 2022

KEYWORDS
HNF1A;
IFN signaling pathway;

Abstract Non-alcoholic steatohepatitis (NASH), a progressive form of non-alcoholic fatty liver disease (NAFLD), is characterised by chronic liver inflammation, which can further progress into complications such as liver cirrhosis and NASH-associated hepatocellular carcinoma (HCC) and therefore has become a growing health problem worldwide. The type I interferon

Abbreviations: DAMPs, danger-associated molecular patterns; HCC, hepatocellular carcinoma; HFD, high-fat diet; HNF1A, hepatocyte nuclear factor 1A; IFN, interferon; IRF3, interferon regulator 3; KO, knock out; MOI, multiplicity of infection; NAFLD, non-alcoholic fatty liver disease; NASH, non-alcoholic steatohepatitis; PAMPs, pathogen-associated molecular patterns; PBMC, peripheral blood mononuclear cell; SeV, Sendai virus; STING, stimulator of interferon genes; TBK1, TANK-binding kinase 1; Ub, ubiquitin; VSV, vesicular stomatitis virus; WT, wild type.

* Corresponding author. Cell-gene Therapy Translational Medicine Research Center, The Third Affiliated Hospital, Sun Yat-sen University, Guangzhou, Guangdong 510630, China.
** Corresponding authors. Molecular Cancer Research Center School of Medicine, Sun Yat-sen University, Shenzhen, Guangdong 518107, China.
E-mail addresses: zhangxd39@mail.sysu.edu.cn (X. Zhang), qinyf6@mail.sysu.edu.cn (Y. Qin), zhangq27@mail.sysu.edu.cn (Q. Zhang).
Peer review under responsibility of Chongqing Medical University.
[1] These authors contributed equally to this work.

https://doi.org/10.1016/j.gendis.2022.05.029

Innate immunity;
NAFLD;
TBK1

(IFN) signaling pathway plays a pivotal role in chronic inflammation; however, the molecular mechanisms underlying NAFLD/NASH from the perspective of innate immune response has not yet been fully explored. In this study, we elucidated the mechanisms of how innate immune response modulates NAFLD/NASH pathogenesis, and demonstrated that hepatocyte nuclear factor-1alpha (HNF1A) was suppressed and the type I IFN production pathway was activated in liver tissues of patients with NAFLD/NASH. Further experiments suggested that HNF1A negatively regulates the TBK1-IRF3 signaling pathway by promoting autophagic degradation of phosphorylated-TBK1, which constrains IFN production, thereby inhibiting the activation of type I IFN signaling. Mechanistically, HNF1A interacts with the phagophore membrane protein LC3 through its LIR-docking sites, and mutations of LIRs (LIR2, LIR3, LIR4, and LIRs) block the HNF1A-LC3 interaction. In addition, HNF1A was identified not only as a novel autophagic cargo receptor but also to specifically induce K33-linked ubiquitin chains on TBK1 at Lys670, thereby resulting in autophagic degradation of TBK1. Collectively, our study illustrates the crucial function of the HNF1A-TBK1 signaling axis in NAFLD/NASH pathogenesis via crosstalk between autophagy and innate immunity.

Introduction

The improvement of living standards and sedentary lifestyles has witnessed a concurrent increase in metabolic diseases. The prevalence of non-alcoholic fatty liver disease (NAFLD) is estimated to be approximately 24% worldwide.[1–3] NAFLD is a "silent" but aggressive disorder that can develop into non-alcoholic steatohepatitis (NASH). Although hepatic steatosis is considered benign and reversible, once inflammation is established, it leads to an increased risk of steatohepatitis, fibrosis, cirrhosis, and eventually hepatocellular carcinoma (HCC).[4] Numerous reports have identified that innate immune networks can regulate the inflammatory response and metabolic activity, thereby facilitating the progression of steatosis to steatohepatitis, liver fibrosis, cirrhosis, and carcinoma.[5,6]

Type I IFN signaling is frequently activated during systemic metabolic disturbances.[7] Emerging studies suggest that initiation and development of NAFLD/NASH are closely correlated with metabolic and inflammatory disarrangements resulting from persistent activation of the innate immune system.[5,6,8] IFN via the interferon α receptor (IFNαR) induces interferon stimulatory gene (ISG) expression, and it has been reported that IFNαR1-deficient mice are protected from high fat diet (HFD)-induced fatty liver and insulin resistance (IR).[7] In addition, researchers have identified several single nucleotide polymorphisms (SNPs) within the IFN region, which play an important role in NAFLD—NASH transition.[9,10] Collectively, these studies show that innate immune responses play an important role in the pathogenesis of steatohepatitis. However, the exact molecular mechanisms of how the IFN signaling pathway modulates steatohepatitis are still not fully understood.

Innate immune response activation is initiated by PAMPs or DAMPs such as various hepatic viruses and free fatty acids (FFAs).[11] The adaptor proteins, including MAVS, STING, and TRIF, activate the downstream protein kinase TBK1 (TANK-binding kinase 1), thereby licencing IRF3 for phosphorylation, which leads to the activation of type I IFN production.[12,13] TBK1 is a key kinase involved in type I IFN signaling activation. In addition to its role in antiviral immunity, TBK1 also acts as an effector of inflammatory signaling in metabolic diseases. Moreover, TBK1 activity increases during obesity and functions as a rheostat to influence the fate of fatty acids in hepatocytes by inducing β-oxidation in the inactive state and promoting re-esterification in the activated state.[14] Although the regulatory network is known, the molecular mechanisms by which components other than adaptor proteins activate TBK1 and IRF3 remain unknown.

Hepatocyte nuclear factor-1alpha (HNF1A), an essential transcription factor, functions predominantly in liver metabolism homeostasis.[15] Mutations in HNF1A are well recognized in hereditary diabetes mellitus. Moreover, patients with HNF1A mutations exhibit hyperglycemia and islet β-cell dysfunction, thereby reducing insulin secretion.[16,17] Therefore, its role in metabolic disorders has attracted increasing attention. HNF1A KO mice reportedly displayed lipid accumulation in the liver and were accompanied by the upregulation of inflammatory cytokines, inciting a chronic low-grade inflammation microenvironment and consequently resulting in metabolic disease progression.[18,19] However, little is known about whether and how HNF1A suppresses steatohepatitis by regulating the type I IFN signaling pathway.

In this study, following a series of molecular approaches, we made an attempt to clarify the detailed mechanism of how HNF1A suppresses the type I interferon signaling pathway by targeting active TBK1 for autophagy degradation. Furthermore, we confirm their consistency with clinical specimens and suggest a potential therapeutic target to prevent steatohepatitis.

Materials and methods

Chemical and reagents

Detailed information on chemical and reagents is presented in Table S1.

Human tissues samples

Human liver samples were obtained from unserviceable grafts after liver transplantation at the Third Affiliated Hospital of Sun Yat-sen University. The experiments were conducted as per the research board protocol of the medical ethical committees of the Third Affiliated Hospital of Sun Yat-sen University. Informed consent was obtained from all subjects and the experiments conform to the principles set out in the WMA Declaration of Helsinki and the Department of Health and Human Services Belmont Report. Information on patients with NAFLD/NASH is presented in Table S2.

Cell culture

HEK293T and *BECN* and *TBK1* KO 293T cells, HepG2, and L02 cells were cultured in Dulbecco's Modified Eagle Medium supplemented with 10% foetal bovine serum. In addition, the THP-1 and PBMCs cells were maintained in RPMI 1640 medium supplemented with 10% FBS. All cells were maintained in a humidified 5% CO_2 atmosphere at 37 °C.

Transfection of plasmids and siRNA

Plasmids were transfected into HEK293T cells using Lipofectamine 3000 (Invitrogen) according to the manufacturer's protocol. Small interfering RNA (siRNA) was purchased from TranSheepBio and transfected into THP-1 cells using Lipofectamine 3000 according to the manufacturer's protocol. The sequences of HNF1A and negative control siRNAs are provided in Table S3.

Generation of knockdown and knockout cell lines

Lentiviruses targeting HNF1A [sh#1, sh#2, sh#3, overexpression (OE)] and a negative control short hairpin RNA (shRNA; NC) were generated with either shRNA or cDNA that had been packaged into HEK293T cells using pMD2.G and psPAX2 plasmids. The medium was changed the next day, and the conditioned medium was collected 48 h after transfection and then used to infect target cells with Polybrene. *BECN* KO and *TBK1* KO cells, target sequences were cloned into pLentiCRISPRv2 by cutting with BsmBI. Stable cell lines were purified by selection with puromycin (10 μg/mL).

Quantitative real-time PCR

Total RNA was isolated with Trizol reagent (Invitrogen) and reverse-transcribed with HiScript II Q RT SuperMix for qPCR (+gDNA wiper) (Vazyme, R223-01). qRT-PCR assays were used to analyse relative mRNA levels using AceQ® qPCR SYBR Green Master Mix (Vazyme). The amount of mRNA for each gene was normalised to 18s. Sequences of primers used in this study are listed in Table S4.

Immunoprecipitation and immunoblot analysis

For immunoprecipitation, whole-cell lysis was carried out by incubating the cells overnight with the corresponding antibodies and Protein A/G beads (Pierce). For immunoprecipitation with anti-FLAG, whole-cell lysis was performed by incubating the cells overnight with anti-Flag agarose gel (Sigma). The beads were then washed six times with low salt lysis buffer. The isolated protein was then eluted with 1 × SDS loading buffer, separated by SDS-PAGE (10%), and transferred to a PVDF membrane. Then, incubated with the appropriate antibodies (TBK1, HNF1A, HA, and Flag) and membranes were detected using enhanced chemiluminescence (ECL) detection system. The antibodies used in this study are listed in Table S5.

Immunofluorescence

293T cells were cultured on glass-bottom culture dishes (Nest Scientific) and treated with Sendai virus (SeV) for 12 h. Cells were then fixed with 4% paraformaldehyde for 20 min and then permeabilized with 0.3% Triton X-100 in 3% bovine serum albumin (BSA) for 10 min. After washing with PBS for two times, cells were blocked in 3% BSA for 1 h. Subsequently, the cells were incubated with a primary antibody against TBK1 and HNF1A overnight at 4 °C, which were then labelled with the appropriate secondary antibody and DAPI-stained for 1 h at room temperature. Images were captured using a microscope.

Luciferase reporter assays

293T cells were seeded in 24-well plates (2 × 10^5/well). Then, these cells were transfected with plasmids encoding the IFN-stimulated response element (ISRE) or IFN-β luciferase reporter (firefly luciferase; 100 or 50 ng) and pRL-TK (Renilla luciferase plasmid; 10 ng) together with 200 ng plasmid encoding Flag-RIG-I (CARD), Flag-MAVS, Flag-TBK1, Flag-IKKi, and Flag-IRF3 (5D) and various doses of plasmid encoding Myc-HNF1A (0, 200, 400). An empty vector (EV) was used to maintain the DNA balance between the wells. Next, the cells were treated with SeV or stimulated with poly(I:C) for the corresponding time points. Luciferase activity was measured using a Dual-Luciferase Reporter Assay System (Promega) with a Luminoskan Ascent luminometer (TECAN). Reporter gene activity was normalised to Renilla luciferase activity.

Oil Red O and Bodipy staining

HepG2 and L02 cells were fixed in 4% paraformaldehyde for 15 min and then washed twice with PBS. They were then stained with 60% Oil Red O (Sigma, O0625) isopropanol solution or 0.1% Bodipy (Molecular Probes, D-3821) PBS solution for 1 h, with extensive washing between every step. Images were captured using a microscope.

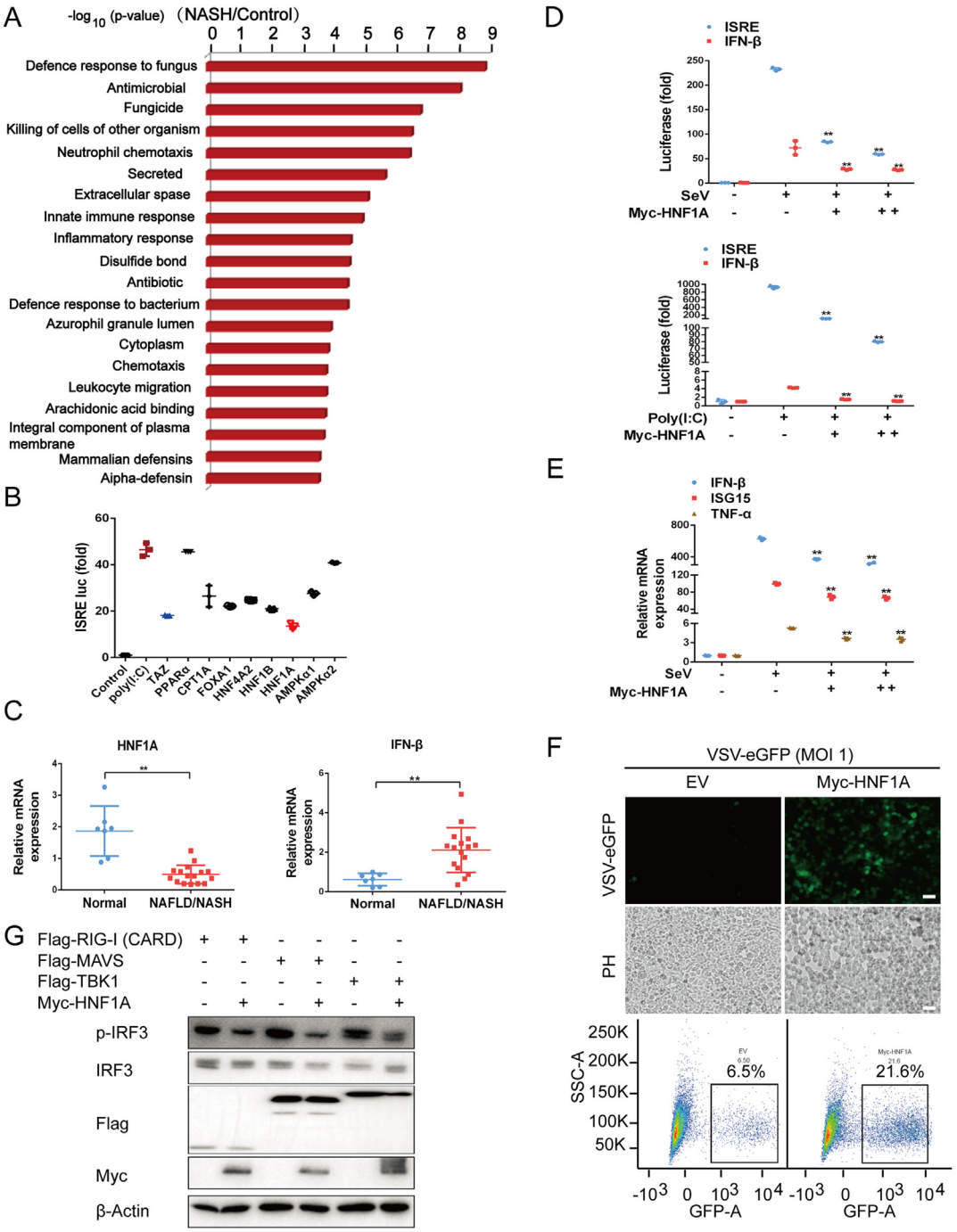

Figure 1 HNF1A negatively regulates type I interferon (IFN) signaling in NASH and innate immunity. **(A)** Enriched pathway RNA-seq reads in normal liver and NASH from the Gene Expression Omnibus (GEO) dataset ($n = 7$ normal livers and 8 NASH). **(B)** Reporter screening of the genes related to liver metabolism indicated HNF1A to be a strong suppressor of type I IFN signaling. 293T cells with expression of ISRE luciferase reporter and various candidate genes were transfected with poly(I:C) for 12 h. **(C)** mRNA levels of HNF1A, and IFN-β derived from healthy human liver and NAFLD/NASH patients. **(D)** Luciferase activity in 293T cells co-transfected with a luciferase reporter for ISRE (ISRE-luc) or IFN-β (IFN-β-luc, 50 ng each) and together with empty vector or Myc-HNF1A (0, 200, and 400 ng), followed by treatment with SeV or poly(I:C) or no treatment (control), results are relative to Renilla luciferase activity. **(E)** 293T cells transfected with empty vector or Myc-HNF1A for 12 h mRNA levels of IFN-β, ISG15, TNFα after SeV infection. **(F)** Phase-contrast (PH) and fluorescence microscopy and flow cytometry detecting the infection of 293T cells transfected with empty vector or Myc-HNF1A, and then infected with VSV-eGFP at an MOI of 1. Original magnification × 10. Numbers above squares indicate percent cells expressing eGFP (infected cells). **(G)** Immunoblot analysis of p-IRF3 and IRF3 in 293T cells transfected with various plasmids for Flag-RIG-I (CARD), Flag-MAVS or Flag-TBK1 plus Myc-HNF1A.

RNA-seq dataset analysis

The Gene Expression Omnibus (GEO) NASH RNA-seq dataset (GSE37031) was downloaded, and differential gene expression analysis of NASH and healthy specimens was performed using DeSeq (Bioconductor Version 2.12). Additionally, the genes that showed significant differences in their expression were classified according to the functional enrichment pathway analysis by DAVID.

Virus infection

SeV, HSV-1 and VSV-eGFP were kindly provided by Dr. Jun Cui (Sun Yat-sen University). HSV-1, Sendai virus, and VSV were propagated on Vero cells. The cells were stimulated with different multiplicities of infection (MOIs), as previously described.[20]

Statistical analysis

Results are presented as the mean ± SEM. Student's *t*-test (two-tailed, unpaired) or one-way ANOVA (three-tailed or more, unpaired) was used to compare the control and treatment groups. The differences with $P < 0.05$ were considered significant.

Results

HNF1A negatively regulates type I IFN signaling in NASH and innate immunity

To explore how inflammation affects the initiation and progression of NAFLD/NASH, we first performed a gene set analysis in NASH and healthy patient specimens using Gene Expression Omnibus (GEO) RNA-sequencing data. We identified that the "innate immune defense response group and inflammatory response group" contained the most increased gene sets in NASH. Further functional enrichment pathway analysis revealed that the identified genes were markedly enriched for defense response, innate immune response, and inflammatory response signaling (Fig. 1A). These results suggest that innate immune response and inflammatory response was overactivated in NASH. In patients with NASH, this condition is usually accompanied by abnormal hepatic glycolipid metabolism. Moreover, type I interferons are the central effectors of innate immunity. Therefore, we hypothesised that genes involved in liver metabolism might participate in type I IFN signaling. Furthermore, to evaluate the possible roles of transcription factors or genes related to liver metabolism in innate immune responses, we generated HEK293T cells expressing an ISRE luciferase reporter and the internal control Renilla luciferase, as well as expression of vectors including candidate genes, and then transfected the cells with poly(I:C) to induce type I IFN signaling. Notably, TAZ is considered a positive control in screening[21] (Fig. 1B). Interestingly, reporter screening indicated that HNF1A, a pivotal transcription factor of the hepatocyte nuclear factor (HNF) family involved in maintaining systemic metabolism homeostasis, significantly hindered type I IFN signaling (Fig. 1B). Subsequently, we detected the mRNA expression of HNF1A and IFN-β in both healthy and NAFLD/NASH clinical liver specimens. Interestingly, the mRNA expression of HNF1A was significantly decreased in NAFLD/NASH compared to that in healthy patients (Fig. 1C), while mRNA expression of IFN-β was remarkably increased in NAFLD/NASH (Fig. 1C). Altogether, these results indicate that NAFLD/NASH exhibits aberrant activation of type I IFN signaling, and HNF1A may mediates the cross-talk between metabolism inflammation and innate immunity. Based on these phenotypes, we then used both ISRE and IFN-β luciferase reporters to further assess the effect of HNF1A on the inhibition of type I IFN signaling. Overexpression of HNF1A significantly decreased the SeV-and intracellular poly(I:C)-induced activity of ISRE and IFN-β luciferase reporters (Fig. 1D). Moreover, overexpression of HNF1A decreased the mRNA expression of IFN-β, TNF-α, and ISG15 in response to SeV infection (Fig. 1E). Next, HNF1A was overexpressed in 293T cells and treated with vesicular stomatitis virus tagged with an enhanced green fluorescent protein (VSV-eGFP) at an MOI of 1. The results indicated that overexpression of HNF1A promoted the cells' sensitivity to viral infection and led to the production of considerably more GFP^+ cells than cells transfected with the empty vector (Fig. 1F). These results imply that HNF1A is a negative regulator of type I IFN signaling.

To address how HNF1A inhibits type I IFN signaling, 293T cells were co-transfected with HNF1A, RIG-I (CARD), MAVS, or TBK1. It was found that HNF1A inhibited the phosphorylation of endogenous IRF3 activated by these cytosolic RNA sensors and adaptors (Fig. 1G). Simultaneously, HNF1A slightly decreased the phosphorylation of endogenous IRF3 activated by the cytosolic DNA adaptor STING (Fig. S1A). Taken together, these results reveal that HNF1A hinders the production of type I IFN, thereby exhibiting a biological function in innate immunity and NASH.

Knockdown of HNF1A promotes IFN-β production as well as innate immune responses

To further investigate the function of HNF1A in regulating innate immune responses, we used two HNF1A-specific siRNAs, and two HNF1A-specific lentivirus RNA (shRNA) constructs to knockdown the expression of HNF1A. All these efficiently decreased the expression of HNF1A in THP-1 and 293T cells (Fig. S1B, C). HNF1A-knockdown in THP-1 cells substantially enhanced the phosphorylation levels of endogenous IRF3 (p-IRF3) under SeV, VSV-eGFP and DNA virus HSV-1 infection (Fig. 2A, B; Fig. S1D), but were not significantly increased under HT-DNA infection (Fig. S1E). Similar results were obtained in 293T cells after infection with SeV (Fig. S1F). Consistently, siRNA-or shRNA-mediated knockdown of HNF1A resulted in higher expression of IFN-β, IFIT1 and ISG15, after infection with SeV (Fig. 2C; Fig. S1G). Similarly, silencing of HNF1A slightly promoted the mRNA expression of IFN-β, IFIT1 and ISG15, upon HSV-1 infection (Fig. S1H). Next, we evaluated the function of HNF1A in innate immunity by knocking down HNF1A in THP-1 cells and then infected them with VSV-eGFP or HSV-1-eGFP at an

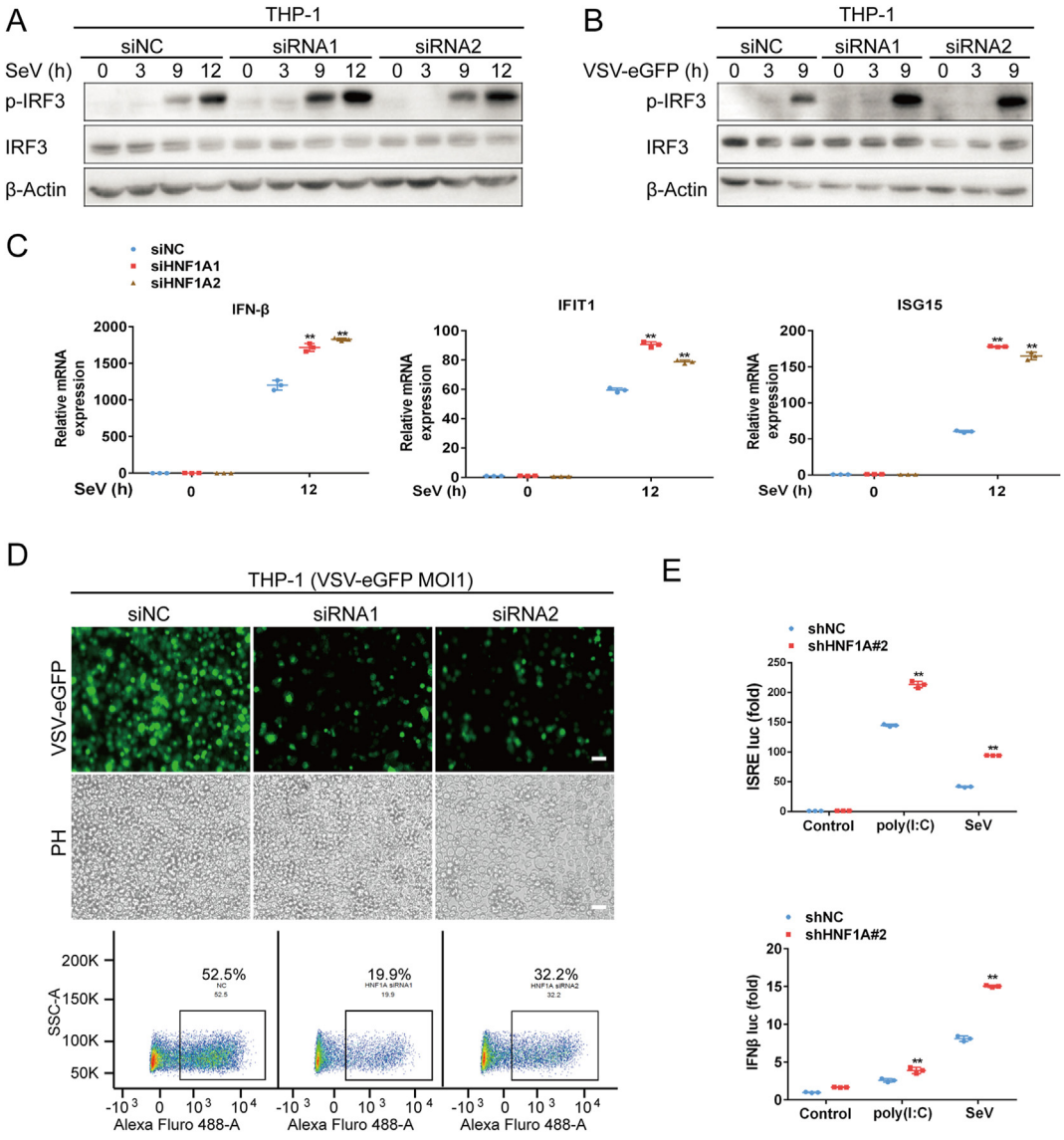

Figure 2 Knockdown of HNF1A promotes innate immune responses. **(A)** THP-1 cells were transfected with NC or HNF1A-specific siRNA, followed by treatment with SeV (MOI 1) at different time points; the lysates were analyzed with indicated antibodies (p-IRF3, IRF3 and β-Actin). **(B)** THP-1 cells were transfected with NC or HNF1A-specific siRNA, followed by treatment with VSV-eGFP (MOI 1) at different time points; the lysates were analyzed with indicated antibodies (p-IRF3, IRF3 and β-Actin). **(C)** THP-1 cells were transfected with NC or HNF1A-specific siRNA, followed by treatment with SeV (MOI 1) at different time points. Relative expressions of IFN-β, IFIT1, and ISG15 mRNA were detected by real-time PCR. **(D)** Phase-contrast (PH) and fluorescence microscopy and flow cytometry detecting the infection of THP-1 cells transfected with NC or HNF1A-specific siRNA and then infected with VSV-eGFP at an MOI of 1. Original magnification × 10. Numbers above squares indicate percent cells expressing eGFP (infected cells). **(E)** HNF1A-knockdown or negative control (shNC) 293T cells transfected with ISRE or IFN-β luciferase reporter, then treated with poly(I:C) or SeV.

MOI of 1. Replication of VSV and HSV-1 in THP-1 cells was detected by green fluorescence protein (GFP) tag integration into the genome, which indicated a significant reduction in VSV and HSV-1 infection when HNF1A expression was abolished (Fig. 2D; Fig. S1I). In addition, luciferase reporter assays revealed that abrogation of HNF1A resulted in markedly higher activity of both the ISRE and IFN-β luciferase reporter induced by SeV or poly(I:C) (Fig. 2E). Taken together, these results suggest that knockdown of HNF1A promotes type I IFN responses.

HNF1A associates with TBK1 and inhibits IRF3 activation

To demonstrate the detailed molecular mechanisms by which HNF1A suppresses type I IFN signaling, we assessed ISRE and IFN-β luciferase reporter activities. The results revealed that HNF1A inhibited the luciferase reporter activity induced by RIG-I (CARD), MAVS, TBK1, IKKi, and STING and weakly inhibited the activity of either luciferase

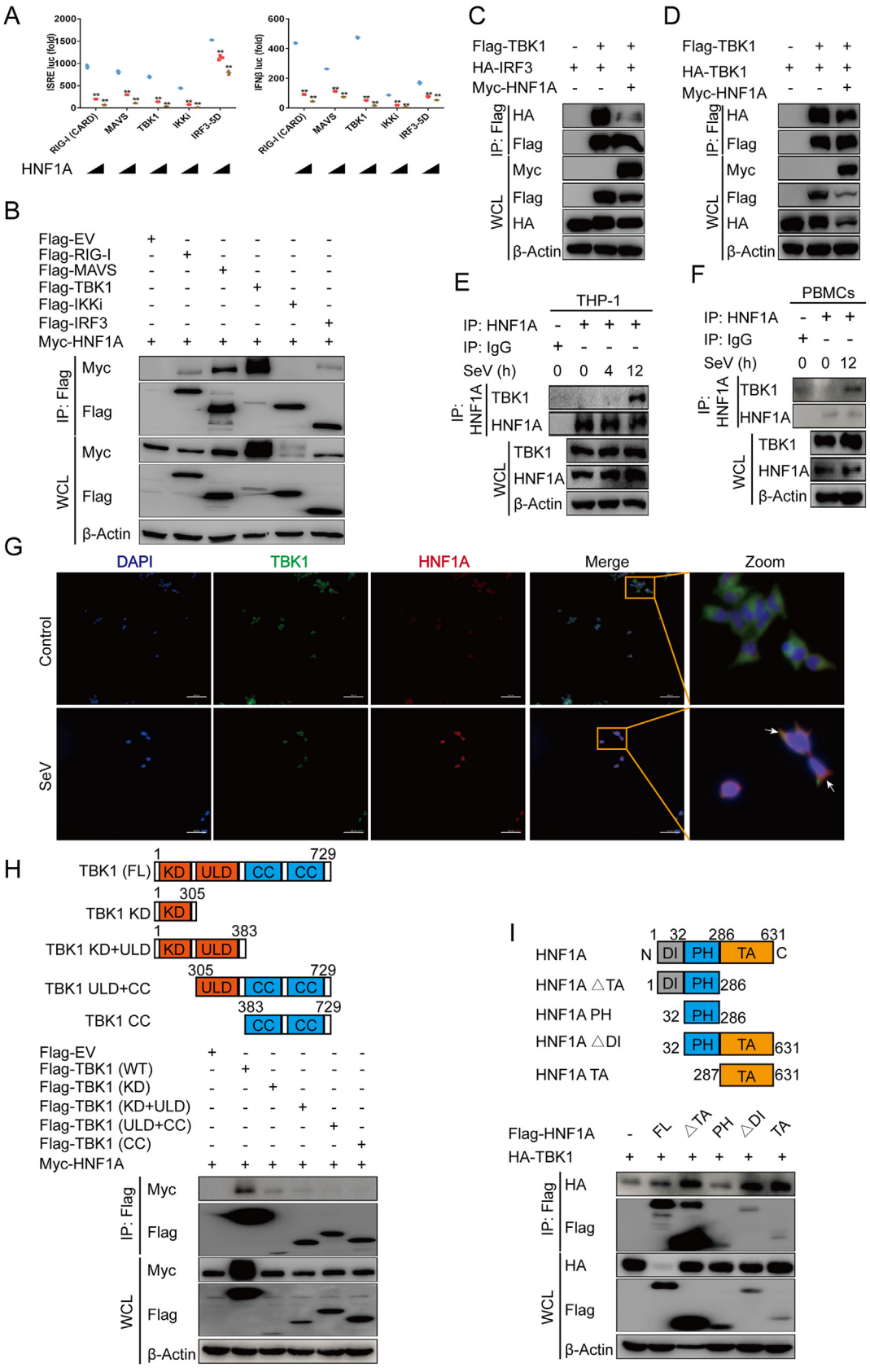

Figure 3 HNF1A interacts with TBK1 to disrupt IRF3 activation. **(A)** 293T cells were transfected with ISRE and IFN-β luciferase reporter, together with RIG-I (CARD), MAVS, TBK1, IKKi or IRF3-5D along with empty vector or increasing amounts of an expression vector for Myc-HNF1A. **(B)** 293T cells were co-transfected with vector for Myc-HNF1A and Flag-EV, Flag-tagged RIG-I, TBK1, MAVS,

reporter induced by IRF3-5D (a constitutively active mutant of IRF3) (Fig. 3A; Fig. S2A). These results suggest that HNF1A might inhibit type I IFN signaling by interacting with signaling molecules within the type I IFN signaling upstream of IRF3. Furthermore, co-immunoprecipitation (co-IP) and immunoblot assays showed that Flag-tagged TBK1 strongly interacted with Myc-HNF1A (Fig. 3B). Consistently, the negative regulation of HNF1A on type I IFN signaling was further tested by surveillance of the interaction of TBK1 with its substrate IRF3 and the oligomerization of TBK1. As expected, HNF1A markedly inhibited the association between TBK1 and IRF3 (Fig. 3C). Similarly, HNF1A also inhibited TBK1 oligomerization (Fig. 3D). In addition, our luciferase and co-immunoprecipitation results suggest that IRF3 might be another target of HNF1A, and to rule out this possibility, we treated THP-1 cells with SeV. Co-immunoprecipitation (co-IP) and immunoblot assays showed that endogenous association between HNF1A and IRF3 did not exist (Fig. S2B). Furthermore, HNF1A knockdown did not affect IRF3 expression under SeV infection (Fig. S2C). These results indicate that IRF3 is not a valid target of HNF1A. Next, to determine whether the association between HNF1A and active form of TBK1 existed during activation of type I IFN signaling, we treated THP-1, PBMCs, and 293T cells with SeV and obtained cell lysates at various time points. The results showed that the endogenous association between HNF1A and TBK1 was enhanced after SeV infection (Fig. 3E, F; Fig. S2D). Furthermore, the co-localization between TBK1 and HNF1A was notably enhanced after SeV stimulation (Fig. 3G). Taken together, these results indicate that HNF1A may interact with the active form of TBK1 in the process of innate immune activation.

To confirm this possibility, we constructed several deletion mutants of TBK1 to investigate the indispensable domains of TBK1 that mediate its association with HNF1A. The results showed that TBK1 mutants involving only the kinase domain (KD) interacted with HNF1A, whereas TBK1 mutants involving the coil—coil domain (CC) or the CC domain plus ubiquitin-like domain (ULD) exhibited no association with HNF1A (Fig. 3H). These results suggest that the kinase domain of TBK1 is essential for HNF1A-TBK1 interaction. HNF1A includes a short N-terminal dimerisation domain (DI), a DNA-binding domain (PH), and a transactivation domain (TA). To determine which domain of HNF1A is required for the association between HNF1A and TBK1, we generated four deletion mutants of HNF1A incorporating only the DNA binding domain (PH), transactivation domain (TA), dimerisation plus DNA binding domain ($\triangle$TA), and DNA binding plus transactivation domain ($\triangle$DI). Co-immunoprecipitation (co-IP) assays demonstrated that TA (287—631), $\triangle$TA (1—286), and $\triangle$DI (32—286) interacted with full-length TBK1, while simultaneous deletion of DI and TA domains disrupted their interaction (Fig. 3I). These data indicate that dimerisation (DI) and transactivation (TA) domains are required for the HNF1A-TBK1 association.

HNF1A mediates the degradation of active TBK1

Next, to investigate how HNF1A inhibits type I IFN signaling activation through its association with TBK1, we co-transfected plasmids encoding Flag-tagged IRF3 with hemagglutinin (HA)-tagged TBK1 into 293T cells, together with increasing amounts of HNF1A. The results showed that the level of TBK1 protein decreased significantly with increasing HNF1A expression (Fig. 4A). Simultaneously, phosphorylation of IRF3 also decreased with increasing doses of HNF1A, accompanied by a decrease in TBK1 (Fig. 4A). To address the possibility that the reduction in TBK1 protein was incited by downregulation of the gene (*TBK1*), qRT-PCR was used to examine the 293T cells. The results revealed that the mRNA level of *TBK1* did not change with increasing expression of HNF1A (Fig. 4B), suggesting that HNF1A might induce TBK1 protein degradation. To verify the specific role of HNF1A-mediated degradation of TBK1, we performed similar experiments in cells expressing RIG-I, MAVS, IKKi, and IRF3 with increasing doses of HNF1A and revealed that HNF1A did not impair the expression of RIG-I, MAVS, IKKi, and IRF3 (Fig. S2E). Furthermore, knockdown of HNF1A arrested the degradation of TBK1 and increased TBK1-induced ISRE and IFN-β luciferase activity (Fig. 4C, D).

It was observed that transfected 293T cells with HNF1A alone did not alter endogenous TBK1 before viral infection (Fig. S2F). As mentioned earlier, because of the association of endogenous active TBK1 with HNF1A upon viral infection, we speculated that HNF1A might induce the active form of TBK1 for degradation. To verify this hypothesis, we transfected 293T cells with HNF1A or empty vector and infected them with VSV-eGFP. The results showed that ectopic expression of HNF1A reduced TBK1 protein in a time-dependent manner after VSV-eGFP infection compared to 293T cells transfected with an empty vector (EV) (Fig. 4E). Conversely, abrogation of HNF1A in THP-1 cells resulted in higher endogenous TBK1 protein levels after infection with SeV or transfection with poly(I:C) (Fig. 4F, G). Similarly,

IKKi or IRF3, followed by immunoprecipitation (IP) with anti-Flag beads and immunoblot analysis with anti-Myc. WCL, immunoblot analysis of whole-cell lysates without immunoprecipitation (throughout). **(C)** 293T cells were co-transfected with Flag-tagged TBK1 and HA-tagged IRF3 with or without Myc-HNF1A, followed by immunoprecipitation (IP) with anti-Flag beads and immunoblot analysis with anti-HA. **(D)** 293T cells were co-transfected with Flag-tagged TBK1 and HA-tagged TBK1 plus Myc-HNF1A or not, followed by immunoprecipitation (IP) with anti-Flag beads and immunoblot analysis with anti-HA. **(E)** THP-1 cells infected with SeV for different time points, followed by immunoprecipitation (IP) with anti-HNF1A and immunoblot analysis. **(F)** PBMCs infected with SeV for different time points, followed by immunoprecipitation (IP) with anti-HNF1A and immunoblot analysis. **(G)** Microscopy of 293T cells treated SeV for 12 h, followed by staining of TBK1 (green) and HNF1A (red) with specific primary antibody. Nuclei were stained with DAPI (blue). Scale bars 100 μm. **(H)** Co-immunoprecipitation and immunoblot analysis of 293T cells transfected with deletion mutants of TBK1 together with Myc-HNF1A. **(I)** Co-immunoprecipitation and immunoblot analysis of 293T cells transfected with deletion mutants of HNF1A together with HA-TBK1.

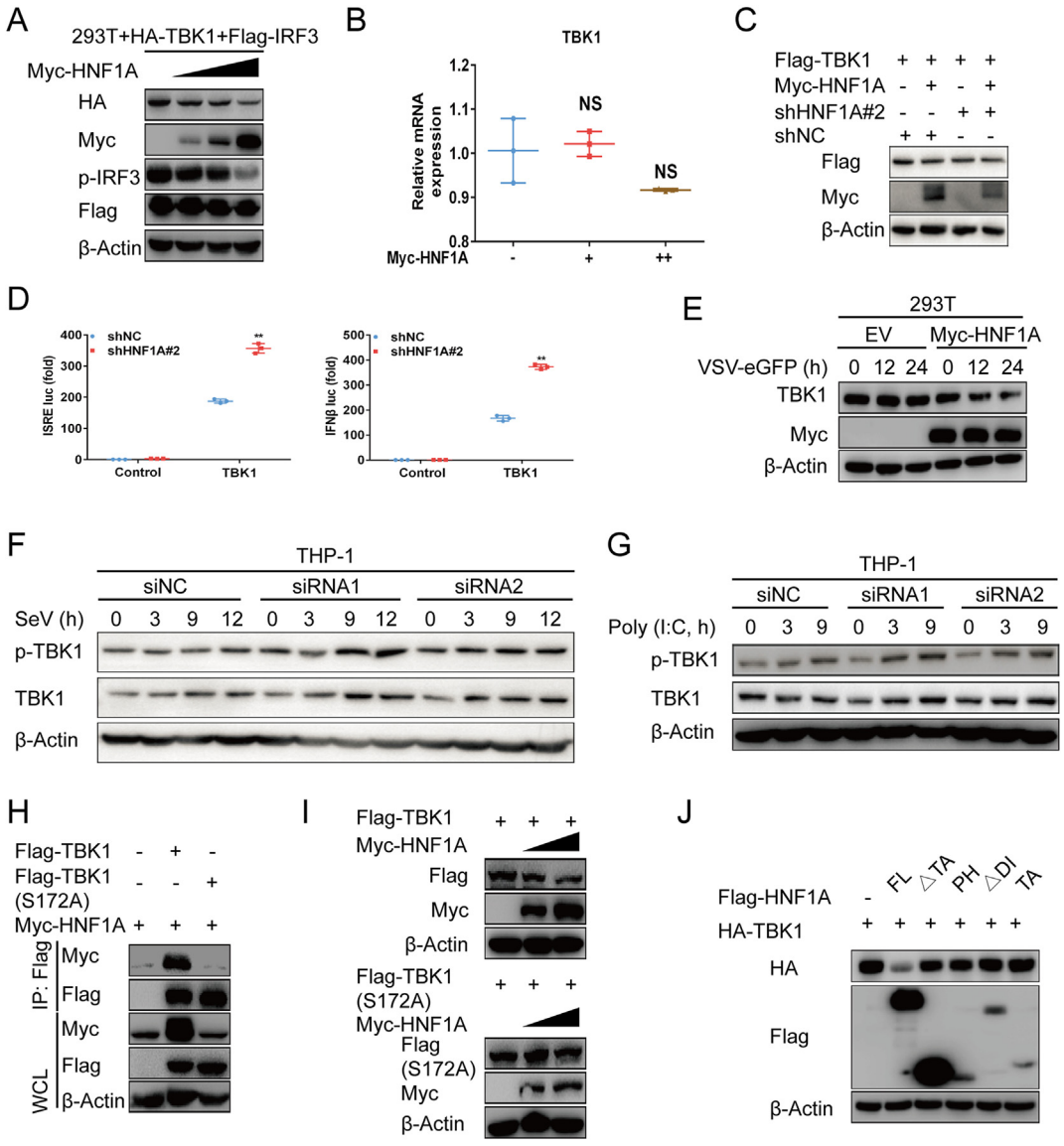

Figure 4 HNF1A mediates the degradation of TBK1. **(A)** Immunoblot analysis of extracts of 293T cells transfected with HA-TBK1 and Flag-IRF3 and increasing doses of Myc-HNF1A. **(B)** 293T cells transfected with various doses of Myc-HNF1A, followed by detection mRNA expression of TBK1 by qRT-PCR. **(C)** Immunoblot analysis of 293T cells transfected with Flag-TBK1 and Myc-HNF1A, as well as HNF1A-specific or control shRNA. **(D)** HNF1A-knockdown or negative control (shNC) 293T cells transfected with ISRE or IFN-β luciferase reporter, followed by reconstitution of TBK1. **(E)** Immunoblot analysis of extracts of 293T cells transfected with Myc-EV or Myc-HNF1A, followed by infection with VSV-eGFP for the indicated time points. **(F)** Immunoblot analysis of extracts of THP-1 cells transfected with NC or HNF1A-specific siRNA, followed by infection with SeV for the indicated time points; the lysates were analyzed with the indicated antibodies (p-TBK1, TBK1 and β-Actin). **(G)** Immunoblot analysis of extracts of THP-1 cells transfected with NC or HNF1A-specific siRNA, followed by infection with poly(I:C) for the different time points; the lysates were analyzed with the indicated antibodies (p-TBK1, TBK1 and β-Actin). **(H)** 293T cells transfected with Myc-HNF1A together with Flag-TBK1 (WT), Flag-TBK1 (S172A). After immunoprecipitation with anti-Flag beads and immunoblot analysis. **(I)** Immunoblot analysis of extracts of 293T cells transfected with Myc-HNF1A together with Flag-TBK1 (WT) or Flag-TBK1 (S172A). **(J)** Immunoblot analysis of 293T cells transfected with deletion mutants of HNF1A together with HA-TBK1.

deletion of HNF1A in THP-1 cells led to much more endogenous TBK1 protein levels upon infection with DNA virus HSV-1 or transfected with HT-DNA (Fig. S2G, H). As HNF1A binds to the kinase domain of TBK1, we next explored whether the interaction between HNF1A and active TBK1 was essential for its degradation. We constructed an inactive mutant of TBK1, which disrupted the phosphorylation of TBK1 with the substitution of alanine for serine at position 172 (S172A). Next, we co-transfected HNF1A, WT TBK1, and TBK1 (S172A) into 293T cells and found that HNF1A interacted with WT TBK1 but did not bind the mutant TBK1 and failed to mediate the degradation in the latter (Fig. 4H, I). Moreover, we found that several deletion mutants of HNF1A failed to promote TBK1 degradation compared to

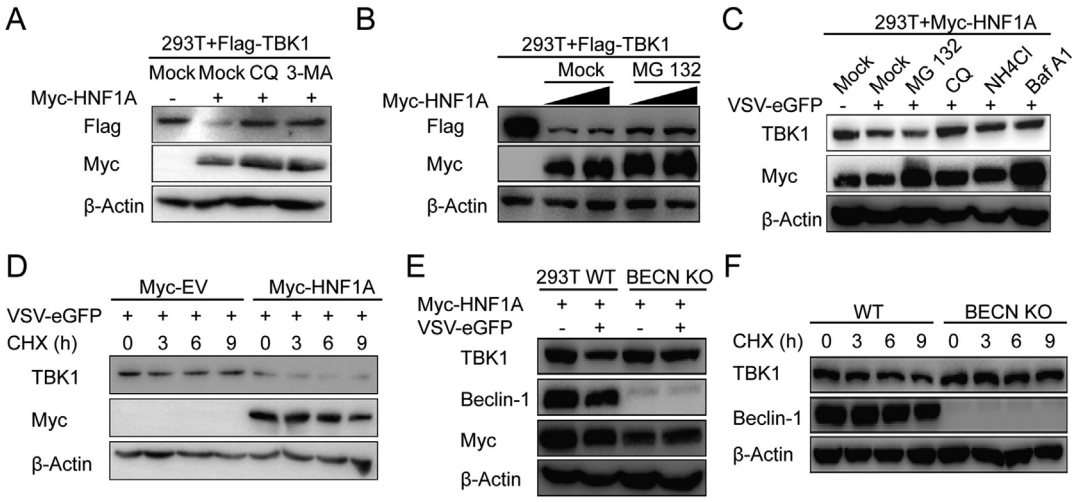

Figure 5 HNF1A promotes the autophagic degradation of TBK1. **(A)** Immunoblot analysis of extracts of 293T cells transfected with Flag-TBK1 and Myc-HNF1A and treated with DMSO, CQ or 3-Methyladenine (3-MA). **(B)** Immunoblot analysis of extracts of 293T cells transfected with Flag-TBK1 and Myc-HNF1A and treated with DMSO or MG 132. **(C)** 293T cells transfected with Myc-HNF1A plasmid for 12 h and then treated or untreated with VSV-eGFP for 12 h. Before collecting, the cells were treated with DMSO, MG 132, CQ, NH_4Cl or Baf A1 for another 12 h; the lysates were analyzed with the indicated antibodies (TBK1, Myc and β-Actin). **(D)** 293T cells transfected with Myc-EV or Myc-HNF1A plasmid for 12 h and then treated with VSV-eGFP. Before collecting, the cells were stimulated with CHX for indicated time points, and the cell lysates were analyzed by immunoblot. **(E)** WT and *BECN* knockout (KO) 293T cells transfected with Myc-HNF1A and then stimulated or unstimulated with VSV-eGFP for 12 h, and the cell lysates were analyzed with the indicated antibodies (TBK1, Beclin-1, Myc and β-Actin). **(F)** WT and *BECN* KO 293T cells were stimulated with CHX for indicated time points, and the cell lysates were analyzed by immunoblot.

full-length HNF1A (Fig. 4J), indicating that the integrity of HNF1A is indispensable for its ability to mediate the degradation of TBK1. These results suggest that HNF1A interacts with the active form of TBK1 (p-TBK1) and specifically promotes its degradation.

HNF1A promotes the autophagic degradation of TBK1

It is well known that protein degradation in eukaryotic cells involves three main pathways: the proteasome, lysosome, and autolysosome pathways.[22,23] Therefore, we investigated the degradation system required for the degradation of TBK1 mediated by HNF1A. The results indicated that the degradation of Flag-TBK1 induced by Myc-HNF1A could be rescued by the autolysosome inhibitor chloroquine (CQ) and autophagy inhibitor 3-methyladenine (3-MA) (Fig. 5A), whereas the proteasome inhibitor, MG 132 could not block the degradation of TBK1 mediated by HNF1A (Fig. 5B), which revealed that HNF1A promoted the degradation of TBK1 via the autolysosome pathway. Similarly, endogenous TBK1 was also decreased by ectopically expressed HNF1A under VSV-eGFP infection, and the lysosome inhibitor NH_4Cl, and the autophagy inhibitors Baf A1 and CQ, rather than MG 132, hindered the degradation of TBK1 (Fig. 5C). Moreover, the TBK1 turnover rates were increased in Myc-HNF1A-overexpressed cells in the presence of translational inhibitor cycloheximide (CHX) when treated with VSV-eGFP (Fig. 5D). These results suggest that HNF1A promotes the autophagic degradation of TBK1. Furthermore, autophagic degradation of TBK1 mediated by HNF1A was rescued in *BECN* KO cells upon VSV-eGFP infection (Fig. 5E). In addition, we found that the rates of TBK1 degradation were impaired in *BECN* KO cells treated with the translational inhibitor cycloheximide (CHX) (Fig. 5F). Altogether, these results indicate that HNF1A promotes autophagic degradation of TBK1.

HNF1A functions as a novel cargo receptor that can bind to LC3

Evidence suggests that cargo receptors play pivotal roles in transferring substrates to the autophagosome for selective autophagic degradation.[24–26] First, we co-transfected Myc-HNF1A and Flag-ATG8 family members (LC3A, LC3B, LC3C, GABARAP, GABARAPL1, GABARAPL2) into 293T cells, and co-immunoprecipitation (co-IP) and immunoblot assays revealed that HNF1A interacted with most of the ATG8 family members (LC3A, LC3C, GABARAP) (Fig. 6A). Furthermore, we transfected Flag-LC3A into 293T cells and observed the interaction between endogenous HNF1A and LC3A (Fig. 6B). Consistent with the above results, we found that the interaction of endogenous HNF1A with LC3 was markedly increased upon SeV infection in THP-1 cells (Fig. 6C). Collectively, these results indicate that HNF1A interacts with LC3 in the process of innate immune activation.

Autophagic cargo receptors can bind to ATG8 family members through a linear peptide sequence called the LC3-interacting region (LIR) and feature core aromatic residue with hydrophobic residues. Through the analysis and prediction by the iLIR Autophagy Database (https://ilir.warwick.ac.uk/), we identified four motifs in human HNF1A (amino acids 32—39, 75—85, 122—134, 178—184)

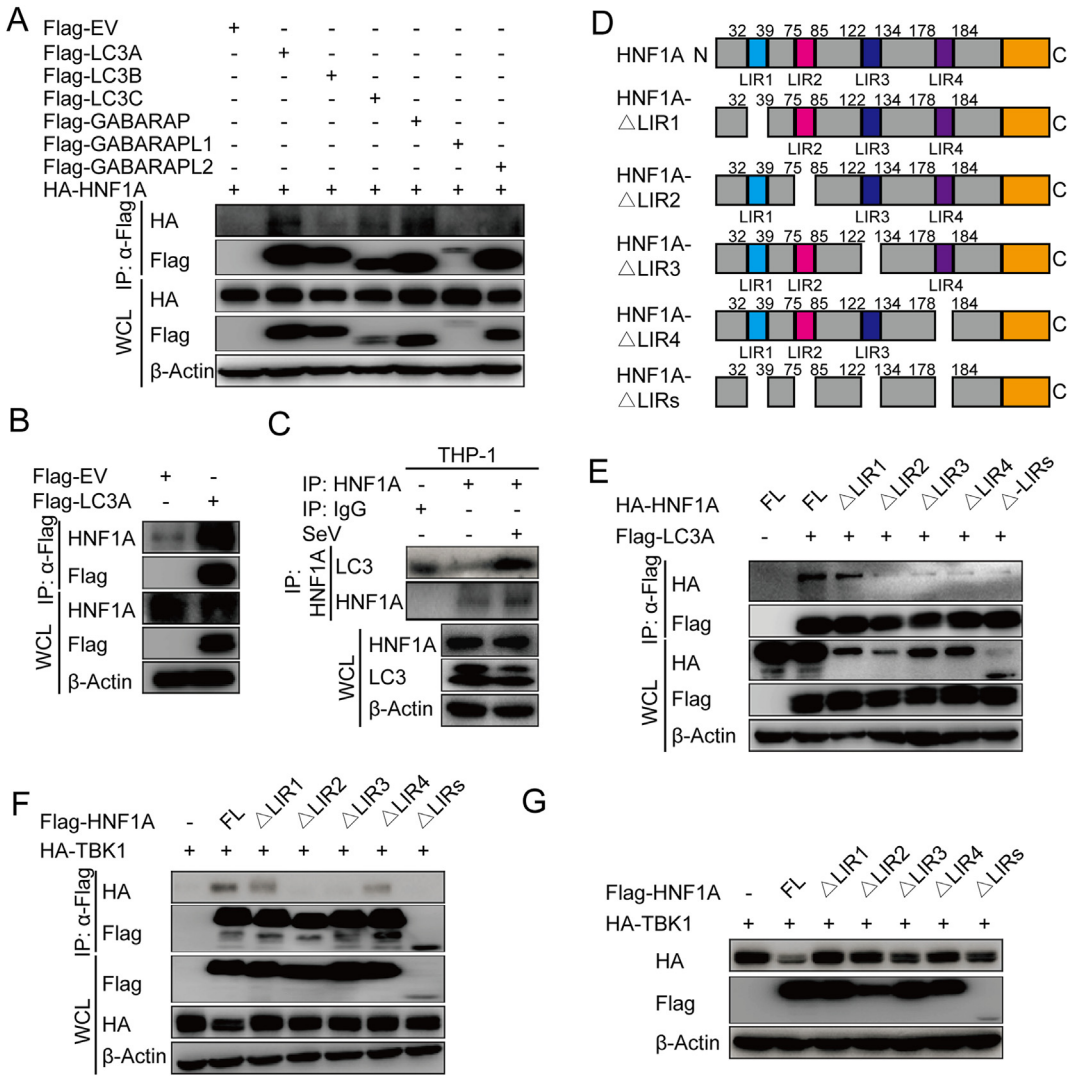

Figure 6 HNF1A can bind to LC3 through its LIR docking sites. **(A)** 293T cells transfected with HA-HNF1A together with Flag-EV, Flag-LC3A, Flag-LC3B, Flag-LC3C, Flag-GABARAP, Flag-GABARAPL1 or Flag-GABARAPL2. After immunoprecipitation with anti-Flag beads and immunoblot analysis. **(B)** 293T cells transfected with Flag-EV or Flag-LC3A, followed by immunoprecipitation (IP) with anti-Flag beads and immunoblot analysis. **(C)** THP-1 cells infected with SeV for 24 h, followed by immunoprecipitation (IP) with anti-HNF1A and immunoblot analysis. **(D)** Schematic diagrams of HNF1A, HNF1A- △LIR1, HNF1A- △LIR2, HNF1A- △LIR3, HNF1A- △LIR4, HNF1A- △LIRs. **(E)** Immunoprecipitation analysis of the interaction between HNF1A and LC3A or its mutants in 293T cells. **(F)** Immunoprecipitation analysis of the interaction between HNF1A and TBK1 or its mutants in 293T cells. **(G)** Immunoblot analysis of 293T cells transfected with deletion mutants of HNF1A together with HA-TBK1.

that were analogous to the well-known LIR sequence (Fig. 6D). Although the predictive LIR motif in human HNF1A did not completely match the canonical LIR (W/Y/FXXL/I/V) sequence, the four motifs (YLLA, FTPP, WRVA, QREV) were hydrophobic. Therefore, we next evaluated whether the LIR motif was indispensable for LC3 association. Five HNF1A mutants, deletion of LIR1, LIR2, LIR3, LIR4, or LIR1 to LIR4, were constructed and named HNF1A- △LIR1, HNF1A- △LIR2, HNF1A- △LIR3, HNF1A- △LIR4 and HNF1A- △LIRs, respectively. Co-IP and immunoblot assays showed that deletion of LIR2 (△aa75-85), LIR3 (△aa122-134), LIR4 (△aa178-184), or LIR1 to LIR4 (LIRs) abrogated the association of HNF1A with LC3A, but HNF1A with a mutation of LIR1 could still interact with LC3A (Fig. 6E). Subsequently, we tested the pivotal amino acids of HNF1A that interacted with TBK1 using different LIR mutants of HNF1A. The results revealed that either HNF1A- △LIR1 or HNF1A- △LIR4 could interact with TBK1, while HNF1A- △LIR2, HNF1A- △LIR3 and HNF1A- △LIRs failed to associate with TBK1 (Fig. 6F). Interestingly, we found that deletion of any LIR motif could disrupt the degradation of TBK1 mediated by HNF1A (Fig. 6G), implying that the LIR motif plays a critical role in TBK1 degradation.

As an autophagic cargo receptor, it degrades with its cargo proteins; thus, we speculated whether endogenous HNF1A was increased by treatment with autophagy in-

hibitors. We found that treatment of cells with Baf A1 resulted in a mildly increase in endogenous HNF1A, but the proteasome inhibitor MG 132 did not affect the HNF1A protein level (Fig. S2I), suggesting that repression of autophagy led to upregulation of HNF1A protein. Altogether, these results reveal that HNF1A functions as a novel autophagic cargo receptor by interacting with LC3 via its LIR motif, thus participating in TBK1 degradation.

HNF1A increases the K33-linked ubiquitination of TBK1 at Lys670

Proteins should be attached to ubiquitin chains before degradation, which serves as an important signal for recognising cargo receptors.[27,28] Therefore, we first tested the polyubiquitination of TBK1 and found that the activation of innate immunity significantly enhanced the polyubiquitination of TBK1 while silencing of HNF1A reduced the polyubiquitination of TBK1 (Fig. 7A). Evidence has suggested that different polyubiquitination processes regulate protein degradation, consisting of K0, K6, K11, K27, K29, K33, K48, and K63-linked ubiquitination.[29,30] Next, we investigated the types of TBK1 ubiquitination that could be caused by HNF1A. Interestingly, we found that HNF1A overexpression significantly induced K33-linked ubiquitination of TBK1 between 8 types of poly-ubiquitination (Fig. 7B). Consistently, we observed that VSV infection markedly induced the K33-linked ubiquitination of TBK1 (Fig. 7C). In contrast, the silencing of HNF1A significantly hampered the K33-linked ubiquitination of TBK1 under VSV infection (Fig. 7D). Altogether, these results indicate that HNF1A induces the autophagic degradation of TBK1 by mediating its K33-linked ubiquitination.

Next, we aimed to determine how HNF1A mediates the K33-linked ubiquitination of TBK1. Therefore, we tested whether HNF1A promoted the K33-linked ubiquitination of TBK1 on the kinase domain (KD) or kinase domain plus ubiquitin-like domain (KD + ULD). The results showed that HNF1A did not affect the ubiquitination of KD or KD + ULD domain (Fig. 7E), which indicated that the carboxyl terminus of TBK1 might be essential for ubiquitination. As previously reported, Lys670 in TBK1 is essential for NLRP4-and USP38 mediated K48-linked ubiquitination and degradation of active TBK1.[31,32] Cui et al recognised three key ubiquitination sites in the carboxyl terminus (coiled-coil domain) of TBK1 by using computer-assisted algorithms.[31] Based on these findings, we hypothesised that HNF1A induces K33-linked ubiquitination and degradation of TBK1 by targeting one of the ubiquitination sites in the coiled-coil domain. Therefore, we generated three mutants of TBK1 by substituting Lys504, Lys661, and Lys670 with arginine (K504R, K661R, K670R; Fig. S3A), and the results suggested that the K670R TBK1 mutant blocked the degradation of TBK1 mediated by HNF1A (Fig. 7F). Simultaneously, the K670R TBK1 mutant did not show an increase in K33-linked ubiquitination mediated by HNF1A, while there was significant HNF1A-mediated K33-linked ubiquitination of wild-type TBK1 (Fig. 7G). Surprisingly, we found that the K670R mutant diminished the K33-linked ubiquitination of TBK1 compared with K504R, K661R TBK1 mutants, and WT TBK1 (Fig. S3B). In addition, we observed that HNF1A could not induce K33-linked ubiquitination of the inactive mutant of TBK1 (S172A), suggesting that the active form of TBK1 is pivotal for HNF1A mediated ubiquitination and degradation (Fig. 7H). Subsequently, we reconstituted WT TBK1 and K670R TBK1 into *TBK1* KO cells, transfected them with or without HNF1A and found that they inhibited phosphorylation of TBK1 and degradation of TBK1 initiated by HNF1A were abrogated in TBK1 K670R reconstituted cells (Fig. S3C). Taken together, these results indicate that HNF1A promotes the degradation of TBK1 and suppresses type I IFN signaling by inducing K33-linked ubiquitination chains of TBK1 at Lys670.

HNF1A can ameliorate NAFLD/NASH via targeting active TBK1

It is well known that HNF1A is a critical transcription factor for the development of liver and plays a crucial role in cell differentiation, metabolism regulation and some other physiological functions.[18,33] In this study, our data revealed that HNF1A was markedly suppressed in NAFLD/NASH liver biopsy specimens (Fig. 8A). Interestingly, we also found that active form of TBK1 (p-TBK1) was significantly upregulated in these samples (Fig. 8A). Therefore, we next studied whether HNF1A could improve NAFLD/NASH by targeting active TBK1.

To further confirm this phenotype in NAFLD/NASH, we established an in vitro NAFLD/NASH model by treating HepG2 or L02 cells with either BSA or BSA-conjugated palmitate. Treatment of HepG2 or L02 cells with palmitate markedly induced the accumulation of lipid droplets, as confirmed by Oil Red O and BODIPY staining (Fig. 8B; Fig. S4A). Consistently, the results showed enhanced phosphorylation of TBK1 and decreased HNF1A protein levels (Fig. S4B), which was consistent with the clinical specimen data. Furthermore, to address the possible interaction between TBK1 and HNF1A in the development of hepatic steatosis, we performed co-IP and immunoblot assays to detect the interaction between TBK1 and HNF1A in the cellular model. The results showed a significant increase in endogenous association between p-TBK1 (active TBK1) and HNF1A after treatment with palmitate (Fig. 8C; Fig. S4C). Notably, we also observed that the association of endogenous HNF1A with p-TBK1 and LC3 was enhanced after palmitate stimulation (Fig. S4D). Taken together, these results indicate that the formation of p-TBK1-HNF1A-LC3 complex after palmitate treatment.

To further evaluate the role of the HNF1A-TBK1 axis in the process of hepatic steatosis, we constructed HNF1A knockdown and overexpression HepG2 cells. Knockdown and overexpression of HNF1A was achieved by using lentiviral shRNAs or cDNA (sh#2, sh#3, and HNF1A OE) and was confirmed by western blotting (Fig. 8D, H). A significant increase of triglycerides (TG) in HNF1A knockdown cells after PA treatment (Fig. 8E). Treatment of HNF1A-knockdown cells with palmitate resulted in increased lipid droplet accumulation, as confirmed by Oil Red O staining (Fig. 8F). Consistent with the above results, knockdown of

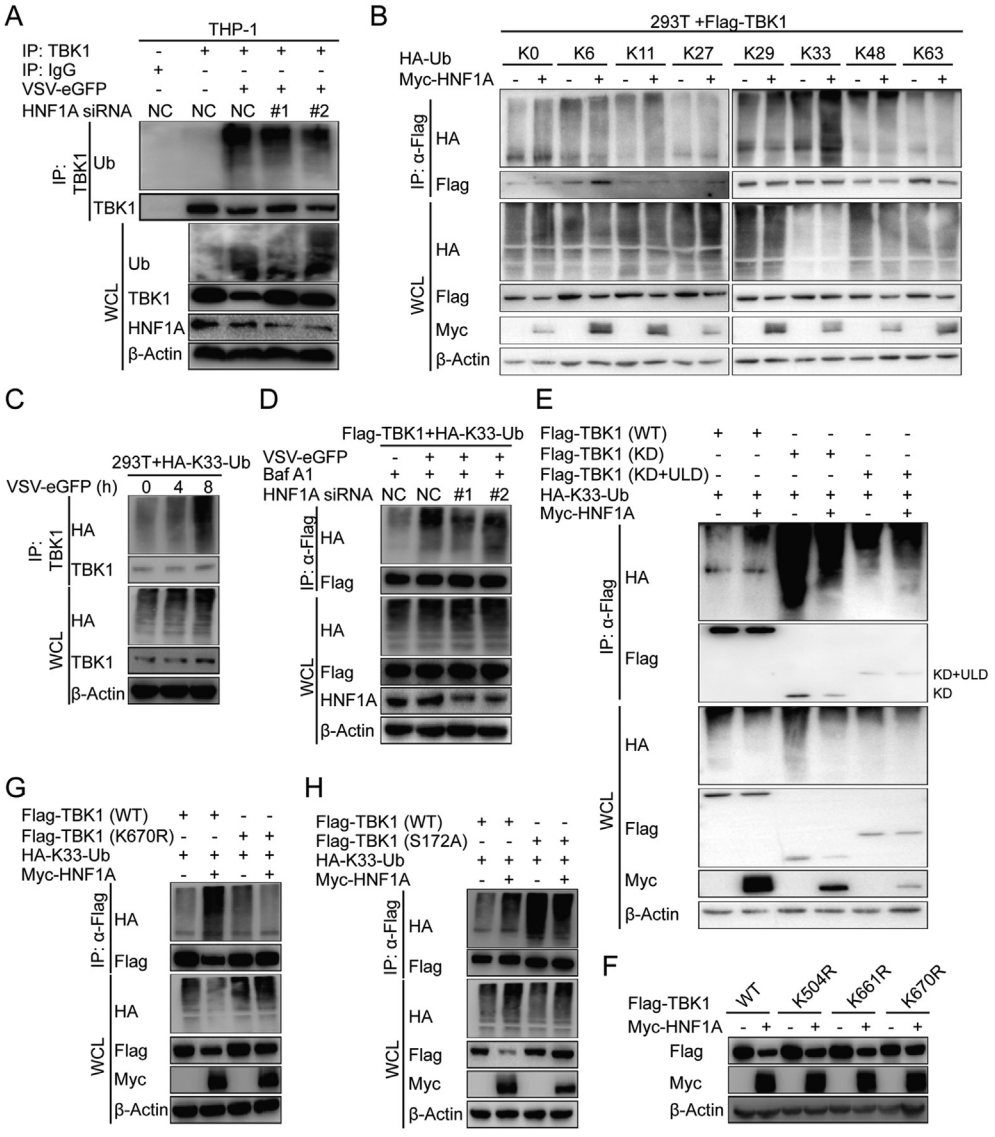

Figure 7 HNF1A induces TBK1 degradation by K33-linked ubiquitination. **(A)** THP-1 cells transfected with NC or HNF1A-specific siRNA and treated with SeV (MOI 1) for indicated time points. Then the lysates were subjected to immunoprecipitation (IP) with anti-TBK1 or IgG as a negative control and immunoblot analysis with indicated antibodies. **(B)** Lysates of 293T cells transfected with Flag-TBK1 and HA-ubiquitin (Ub) and its indicated mutants, along with Myc-EV or Myc-HNF1A, followed by immunoprecipitation with anti-Flag beads and immunoblot analysis. **(C)** 293T cells transfected HA-K33-linked ubiquitin, then infected with VSV-eGFP for the indicated time points, followed by immunoprecipitation with anti-TBK1 and immunoblot analysis with anti-HA. **(D)** 293T cells transfected with HNF1A-specific siRNA and Flag-TBK1, plus ubiquitin K33 mutant, and infected with VSV-eGFP for 24 h. Before collecting, the cells were treated with Baf A1 and immunoprecipitated with anti-Flag and immunoblotted with anti-HA. **(E)** Immunoassay of extracts of 293T cells transfected with Myc-HNF1A and HA-K33-linked ubiquitin together with Flag-TBK1 constructs (as in Fig. 3G), followed by immunoprecipitation with anti-Flag beads and immunoblot analysis with anti-HA. **(F)** Immunoblot analysis of extracts of 293T cells transfected with Myc-EV or Myc-HNF1A, along with Flag-tagged wild type TBK1 or K504R, K661R or K670R mutant of TBK1. **(G)** 293T cells transfected with Myc-HNF1A and HA-K33-linked ubiquitin, plus Flag-TBK1 or Flag-TBK1 (K670R), followed by immunoprecipitation with anti-Flag beads and immunoblot analysis with anti-HA. **(H)** 293T cells transfected with Myc-HNF1A and HA-K33-linked ubiquitin, plus Flag-TBK1 or Flag-TBK1 (S172A), followed by immunoprecipitation with anti-Flag beads and immunoblot analysis with anti-HA.

HNF1A remarkably induced the phosphorylation of TBK1 under treatment with palmitate (Fig. 8G). In contrast, overexpression of HNF1A significantly suppressed the phosphorylation of TBK1 and simultaneously ameliorated excessive accumulation of lipid droplets (Fig. 8H, I). Collectively, these results indicate that the HNF1A-TBK1 axis display an essential biological function in the innate immune response and NAFLD/NASH.

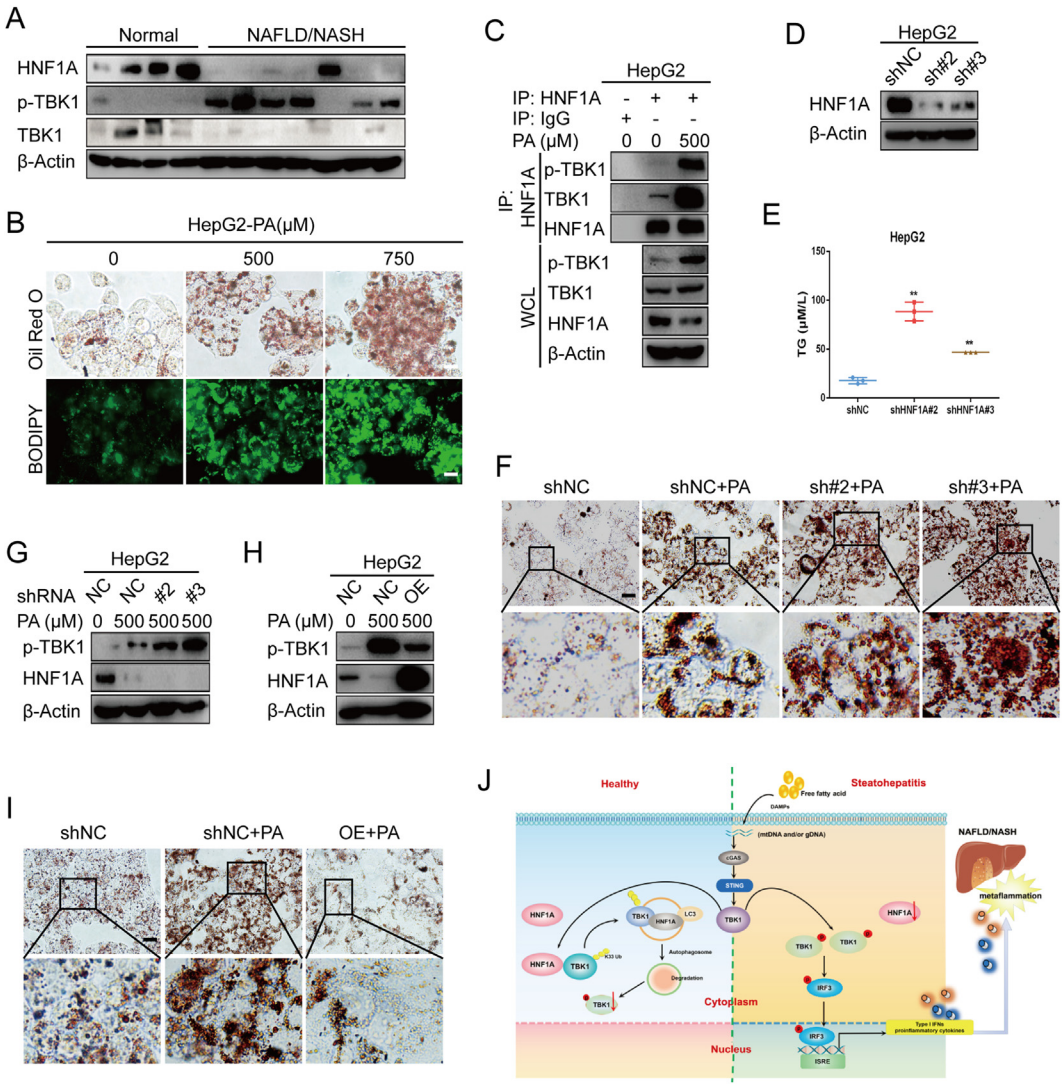

Figure 8 HNF1A ameliorates NAFLD/NASH via targeting active TBK1. **(A)** Immunoblot analysis of phosphorylated TBK1 (p-TBK1) and HNF1A in NAFLD/NASH and normal clinical specimens. **(B)** Representative Oil Red O or BODIPY staining in HepG2 cells challenged with palmitate for 24 h. Original magnification, 20×. **(C)** HepG2 cells treated with BSA or BAS-palmitate for 24 h, followed by immunoprecipitation with anti-HNF1A and immunoblot analysis with p-TBK1 and TBK1. **(D)** HNF1A knockdown (KD) in HepG2 cells at protein levels. **(E)** Triglyceride content quantification in shNC or HNF1A KD HepG2 cell lysates. (F) Representative Oil Red O staining in shNC or HNF1A KD HepG2 cells treated with BSA or BSA-palmitate for 24 h. Original magnification, 20×. **(G)** Immunoblot analysis of phosphorylated TBK1 (p-TBK1) and HNF1A in shNC or HNF1A KD HepG2 cells treated with BSA or palmitate for 24 h. **(H)** Immunoblot analysis of phosphorylated TBK1 (p-TBK1) and HNF1A in shNC or HNF1A overexpression (OE) HepG2 cells treated with BSA or BSA-palmitate for 24 h. **(I)** Representative Oil Red O staining in shNC or HNF1A overexpression (OE) HepG2 cells treated with BSA or BSA-palmitate for 24 h. Original magnification, 20 ×. **(J)** Schematic representation of HNF1A-mediated innate immune responses in the pathogenesis of NAFLD/NASH.

Discussion

NASH is characterised by lipid deposition, metabolic inflammation, and abnormal liver function. It is believed that the innate immune system exerts a profound impact on promoting liver inflammation.[6] Accordingly, the present study demonstrated that the HNF1A-mediated type I IFN signaling plays an important role in NAFLD/NASH. Specifically, we found that HNF1A was suppressed in liver tissues from patients with NAFLD/NASH and was accompanied by persistent activation of the type I IFN signaling. Furthermore, we demonstrated that HNF1A could suppress type I IFN signaling by targeting the active form of TBK1 for selective autophagic degradation. Our results also reveal that HNF1A is a previously uncharacterised cargo receptor that can bind to LC3 in the process of innate immune activation (Fig. 8J). Collectively, this study reveals that HNF1A suppresses NAFLD/NASH from a distinctive perspective.

Previous studies have determined that HNF1A is a canonical transcription factor regulating metabolism and has an important role in NAFLD/NASH. Reportedly, mutations in HNF1A cause diabetes, wherein the HNF1A KO mice have

been shown to suffer from fatty liver-related HCC.[16,33] Aberrant expression of HNF1A usually leads to dysfunction of glucose and lipid metabolism and overproduction of inflammatory cytokines, ultimately resulting in systemic inflammation.[18] For example, the HNF1A gene contains one of the 27 SNPs associated with an increased risk of coronary artery disease (CAD), which is highly correlated with hyperlipemia and metabolic inflammation.[34] Moreover, C-reactive protein (CRP), a pattern-recognition molecule of innate immunity and a biomarker of systemic low-grade inflammation, has been shown to be predictive of future CAD, whereas several studies have demonstrated that HNF1A is indispensable for the expression of CRP.[35,36] In the condition of liver fibrosis, suppression of HNF1A in hepatocytes leads to the activation of NF-κB and JAK/STAT pathways, subsequently initiating an HNF1A-regulated inflammatory feedback loop between hepatocytes and hepatic stellate cells.[19,37] These findings suggest that HNF1A could be an essential element in linking metabolic disorders and innate immune overreactions underlying the pathogenesis of NAFLD/NASH. Although some studies consider HNF1A to be associated with innate immunity, the precise molecular mechanism remains obscure. Interestingly, our study shows that HNF1A negatively regulates type I IFN signaling by inducing autophagic degradation of phosphorylated-TBK1 and suggests that HNF1A not only function as a transcription factor but also as a cargo receptor.

As a cargo receptor, it has two main characteristics: the recognition of the substrate through a specific domain, and the subsequent association with LC3 through the LIR domain.[25] In addition to the classic LIR motif with the consensus sequence W/F/YXXL/I/V, some studies have reported another cargo receptor in eukaryotic cells, which interacts with LC3 through a similar LIR motif structure (hereafter referred to as the noncanonical LIR motif).[38,39] In this study, we demonstrate that HNF1A harbours four noncanonical LIRs, of which LIR2 to LIR4 motifs were indispensable for HNF1A mediated selective autophagic degradation of active TBK1. Collectively, our results reveal a new cargo receptor with non-canonical LIR motifs. Moreover, our results indicate that HNF1A induces the autophagic degradation of TBK1 by mediating its K33-linked ubiquitination. However, HNF1A is not a recognised E3 ubiquitin ligase, so we had to resolve the mechanism of how HNF1A promotes TBK1 polyubiquitination. We hypothesized that HNF1A might act as a scaffold protein to link active TBK1 and its E3 ligases for ubiquitination and degradation. To address this possibility, we performed a literature search and found that online protein—protein interaction (PPI) databases such as GPS-Prot and Integration Interactions Database (IID) show 54 and 56 HNF1A interaction partners: both included the E3 ubiquitin—protein ligase Ring Finger Protein 14 (RNF14).[40,41] Moreover, through the analysis and prediction by BioGRID database (https://thebiogrid.org/), we identified 62 HNF1A interaction partners and RNF14 is one of them (Table S7). Therefore, to evaluate whether RNF14 participates in the regulation of TBK1 mediated by HNF1A, we next examined the association of RNF14 with TBK1 in HNF1A knockdown cells. Surprisingly, we found that HNF1A knockdown reduced the interaction between RNF14 and TBK1 after SeV infection (date not shown), indicating a potential regulatory function of RNF14 in HNF1A-mediated TBK1 ubiquitination. The preliminary results only proved that RNF14 may be involved in the ubiquitination and degradation of HNF1A-mediated TBK1; however, the detailed mechanism still remains unclear. Thus, in further research we need to explain the exact mechanism of RNF14 in the regulation of TBK1 to figure out how HNF1A promotes the polyubiquitination of TBK1.

TBK1 acts as a key adaptor protein in type I IFN signaling and plays an essential role in innate immune responses. Its overactivation results in excessive production of IFNs, thus leading to inflammatory damage. Therefore, to maintain systemic homeostasis, the balance between the active and quiescent state of TBK1 must be tightly regulated under different physiological conditions. Emerging evidence suggests that the stability of TBK1 is mainly controlled by post-translational modifications.[31,32] Numerous studies have identified that several molecules negatively regulate the type I IFN signaling by promoting TBK1 degradation via the proteasome pathway, including NLRP4, USP38, DDX19, DYRK2, SOCS3, and TRIP.[31,32,42–45] Moreover, selective autophagy is also an important pathway for the degradation of key signaling adaptors of the type I IFN signaling. In this study, for the first time, we confirm that HNF1A functions as a selective autophagic cargo receptor that mediates the autophagic degradation phosphorylated-TBK1.

It is well known that TBK1 plays a critical role in antiviral immunity and has been recognised as an effector of inflammatory signaling in metabolic diseases.[46] One study reported that cGAS-STING mediated TBK1 activation in NASH models. Similarly, our findings demonstrated phosphorylated TBK1 levels were upregulated in fatty livers, which attributed to the reduction in its selective autophagic degradation mediated by HNF1A. In contrast, reconstitution of HNF1A suppresses the activity of TBK1 (p-TBK1) and reduces fatty acid accumulation in hepatocytes. Altogether, these results may shed light on designing novel therapeutic targets for the treatment of NAFLD/NASH by modulating the HNF1A-TBK1 axis. However, it is also important to note that this study was conducted in cultured cells and clinical samples, and it would have been improved by having animal models to fully validate these mechanisms. Further study may provide new insights and comprehensive understanding of the signaling mechanism of HNF1A-TBK1.

In conclusion, this study illustrates the pivotal role of HNF1A-mediated innate immune responses in the pathogenesis of NAFLD/NASH (Fig. 8J). Furthermore, our results unveil a deep connection between metabolism and innate immune networks, which is mediated by the HNF1A-TBK1 axis. These could help unmask the pathophysiological mechanisms of NAFLD/NASH.

Author contributions

JH and CD carried out the experiments and analyzed the data. XP, WH, DQ, and XZ contributed to several experiments and involved in discussion of data. QZ, YQ and XZ conceived the study and experimental design. JH, CD and QZ wrote the manuscript.

Conflict of interests

The authors declare no competing conflict of interests.

Funding

This study was supported by the National Natural Science Foundation of China (No. 81970509, 82000620, 81870449 and 81800559), and the Fundamental Research Funds for the Central Universities (No. 20ykzd03 and 19ykpy26).

Acknowledgements

We are grateful to Mao Pang (The Third Affiliated Hospital, Sun Yat-sen University) who provided invaluable help for the graphical abstract. We thank Xinyue Wang and Huijun Qiu (The Third Affiliated Hospital, Sun Yat-sen University) for the kind gift of PBMCs. The last but not the least, the GEO database is highly appreciated.

Appendix A. Supplementary data

Supplementary data to this article can be found online at https://doi.org/10.1016/j.gendis.2022.05.029.

References

1. Loomba R, Friedman SL, Shulman GI. Mechanisms and disease consequences of nonalcoholic fatty liver disease. *Cell*. 2021; 184(10):2537—2564.
2. Younossi Z, Anstee QM, Marietti M, et al. Global burden of NAFLD and NASH: trends, predictions, risk factors and prevention. *Nat Rev Gastroenterol Hepatol*. 2018;15(1):11—20.
3. de Jesus DF, Orime K, Kaminska D, et al. Parental metabolic syndrome epigenetically reprograms offspring hepatic lipid metabolism in mice. *J Clin Invest*. 2020;130(5):2391—2407.
4. Friedman SL, Neuschwander-Tetri BA, Rinella M, Sanyal AJ. Mechanisms of NAFLD development and therapeutic strategies. *Nat Med*. 2018;24(7):908—922.
5. Bai L, Li H. Innate immune regulatory networks in hepatic lipid metabolism. *J Mol Med (Berl)*. 2019;97(5):593—604.
6. Cai J, Xu M, Zhang X, Li H. Innate immune signaling in nonalcoholic fatty liver disease and cardiovascular diseases. *Annu Rev Pathol*. 2019;14:153—184.
7. Ghazarian M, Revelo XS, Nøhr MK, et al. Type I interferon responses drive intrahepatic T cells to promote metabolic syndrome. *Sci Immunol*. 2017;2(10):eaai7616.
8. Yang Q, Liu R, Yu Q, Bi Y, Liu G. Metabolic regulation of inflammasomes in inflammation. *Immunology*. 2019;157(2): 95—109.
9. Weiskirchen R, Wasmuth HE. The genes that underlie fatty liver disease: the harvest has begun. *Hepatology*. 2009;49(2): 692—694.
10. Yi G, Brendel VP, Shu C, Li P, Palanathan S, Kao CC. Single nucleotide polymorphisms of human STING can affect innate immune response to cyclic dinucleotides. *PLoS One*. 2013; 8(10):e77846.
11. Bai J, Liu F. The cGAS-cGAMP-STING pathway: a molecular link between immunity and metabolism. *Diabetes*. 2019;68(6): 1099—1108.
12. Takeuchi O, Akira S. Pattern recognition receptors and inflammation. *Cell*. 2010;140(6):805—820.
13. He Y, Hara H, Núñez G. Mechanism and regulation of NLRP3 inflammasome activation. *Trends Biochem Sci*. 2016;41(12): 1012—1021.
14. Huh JY, Reilly SM, Abu-Odeh M, et al. TANK-binding kinase 1 regulates the localization of acyl-CoA synthetase ACSL1 to control hepatic fatty acid oxidation. *Cell Metab*. 2020;32(6): 1012—1027. e7.
15. Begum S. Hepatic nuclear factor 1 alpha (HNF-1α) in human physiology and molecular medicine. *Curr Mol Pharmacol*. 2020; 13(1):50—56.
16. Bellanné-Chantelot C, Carette C, Riveline JP, et al. The type and the position of HNF1A mutation modulate age at diagnosis of diabetes in patients with maturity-onset diabetes of the young (MODY)-3. *Diabetes*. 2008;57(2):503—508.
17. Yamagata K, Furuta H, Oda N, et al. Mutations in the hepatocyte nuclear factor-4alpha gene in maturity-onset diabetes of the young (*MODY1*). *Nature*. 1996;384(6608):458—460.
18. Tan J, Xu J, Wei G, et al. HNF_1 α controls liver lipid metabolism and insulin resistance via negatively regulating the SOCS-3-STAT3 signaling pathway. *J Diabetes Res*. 2019;2019:5483946.
19. Qian H, Deng X, Huang ZW, et al. An HNF1α-regulated feedback circuit modulates hepatic fibrogenesis via the crosstalk between hepatocytes and hepatic stellate cells. *Cell Res*. 2015; 25(8):930—945.
20. Cui J, Song Y, Li Y, et al. USP3 inhibits type I interferon signaling by deubiquitinating RIG-I-like receptors. *Cell Res*. 2014;24(4):400—416.
21. Zhang Q, Meng F, Chen S, et al. Hippo signalling governs cytosolic nucleic acid sensing through YAP/TAZ-mediated TBK_1 blockade. *Nat Cell Biol*. 2017;19(4):362—374.
22. Liu T, Tang Q, Liu K, et al. TRIM11 suppresses AIM2 inflammasome by degrading AIM2 via p62-dependent selective autophagy. *Cell Rep*. 2016;16(7):1988—2002.
23. Jin S, Tian S, Luo M, et al. Tetherin suppresses type I interferon signaling by targeting MAVS for NDP52-mediated selective autophagic degradation in human cells. *Mol Cell*. 2017;68(2): 308—322. e4.
24. Gatica D, Lahiri V, Klionsky DJ. Cargo recognition and degradation by selective autophagy. *Nat Cell Biol*. 2018;20(3): 233—242.
25. Johansen T, Lamark T. Selective autophagy mediated by autophagic adapter proteins. *Autophagy*. 2011;7(3):279—296.
26. Choi AMK, Ryter SW, Levine B. Autophagy in human health and disease. *N Engl J Med*. 2013;368(7):651—662.
27. Komander D, Rape M. The ubiquitin code. *Annu Rev Biochem*. 2012;81(1):203—229.
28. Shaid S, Brandts CH, Serve H, Dikic I. Ubiquitination and selective autophagy. *Cell Death Differ*. 2013;20(1):21—30.
29. Meng X, Liu X, Guo X, et al. FBXO38 mediates PD-1 ubiquitination and regulates anti-tumour immunity of T cells. *Nature*. 2018;564(7734):130—135.
30. Komander D. The emerging complexity of protein ubiquitination. *Biochem Soc Trans*. 2009;37(Pt 5):937—953.
31. Cui J, Li Y, Zhu L, et al. NLRP4 negatively regulates type I interferon signaling by targeting the kinase TBK_1 for degradation via the ubiquitin ligase DTX4. *Nat Immunol*. 2012;13(4): 387—395.
32. Lin M, Zhao Z, Yang Z, et al. USP38 inhibits type I interferon signaling by editing TBK_1 ubiquitination through NLRP4 signalosome. *Mol Cell*. 2016;64(2):267—281.
33. Patitucci C, Couchy G, Bagattin A, et al. Hepatocyte nuclear factor 1α suppresses steatosis-associated liver cancer by inhibiting PPARgamma transcription. *J Clin Invest*. 2017; 127(5):1873—1888.
34. Zhou YJ, Yin RX, Hong SC, Yang Q, Cao XL, Chen WX. Association of the HNF1A polymorphisms and serum lipid traits, the risk of coronary artery disease and ischemic stroke. *J Gene Med*. 2017;19(1—2):e2941.

35. Sucajtys-Szulc E, Debska-Slizien A, Rutkowski B, et al. Hepatocyte nuclear factors as possible C-reactive protein transcriptional inducer in the liver and white adipose tissue of rats with experimental chronic renal failure. *Mol Cell Biochem*. 2018;446(1—2):11—23.
36. Sara JDS, Prasad M, Zhang M, et al. High-sensitivity C-reactive protein is an independent marker of abnormal coronary vasoreactivity in patients with non-obstructive coronary artery disease. *Am Heart J*. 2017;190:1—11.
37. Ding CH, Yin C, Chen SJ, et al. The HNF1α-regulated lncRNA HNF1A-AS1 reverses the malignancy of hepatocellular carcinoma by enhancing the phosphatase activity of SHP-1. *Mol Cancer*. 2018;17(1):63.
38. von Muhlinen N, Akutsu M, Ravenhill BJ, et al. LC3C, bound selectively by a noncanonical LIR motif in NDP52, is required for antibacterial autophagy. *Mol Cell*. 2012;48(3):329—342.
39. Smith MD, Harley ME, Kemp AJ, et al. CCPG1 is a non-canonical autophagy cargo receptor essential for ER-phagy and pancreatic ER proteostasis. *Dev Cell*. 2018;44(2):217—232. e11.
40. Valkovicova T, Skopkova M, Stanik J, Gasperikova D. Novel insights into genetics and clinics of the HNF1A-MODY. *Endocr Regul*. 2019;53(2):110—134.
41. Kotlyar M, Pastrello C, Sheahan N, Jurisica I. Integrated interactions database: tissue-specific view of the human and model organism interactomes. *Nucleic Acids Res*. 2016;44(D1):D536—D541.
42. Zhang K, Zhang Y, Xue J, et al. DDX19 inhibits type I interferon production by disrupting TBK_1-IKKϵ-IRF_3 interactions and promoting TBK_1 and IKKϵ degradation. *Cell Rep*. 2019;26(5):1258—1272. e4.
43. An T, Li S, Pan W, et al. DYRK2 negatively regulates type I interferon induction by promoting TBK_1 degradation via Ser527 phosphorylation. *PLoS Pathog*. 2015;11(9):e1005179.
44. Liu D, Sheng C, Gao S, et al. $SOCS_3$ drives proteasomal degradation of TBK_1 and negatively regulates antiviral innate immunity. *Mol Cell Biol*. 2015;35(14):2400—2413.
45. Zhang M, Wang L, Zhao X, et al. TRAF-interacting protein (TRIP) negatively regulates IFN-β production and antiviral response by promoting proteasomal degradation of TANK-binding kinase 1. *J Exp Med*. 2012;209(10):1703—1711.
46. Zhao P, Wong KI, Sun X, et al. TBK_1 at the crossroads of inflammation and energy homeostasis in adipose tissue. *Cell*. 2018;172(4):731—743. e12.